Werkdocument

Ministerie van Verkeer en Waterstaat
Directoraat-Generaal Rijkswaterstaat
Rijksinstituut voor Kust en Zee / RIKZ

Aan
MOVE

Van
A. Langerak
Datum
18 april 1997
Nummer
RIKZ/OS-97.812X
Onderwerp
Verdieping Westerschelde
monitoring morfologie

Doorkiesnummer
0118-672282
Bijlage(n)

Project

1. Inleiding

De komende verdieping van de Westerschelde zal het globale hydraulisch en morfologisch gedrag van het estuarium niet wezenlijk veranderen. Toch is het verstandig om dit te monitoren. Voorgesteld wordt om het gedrag dmv de getijasymetrie vast te leggen, omdat dit een zeer kenmerkende parameter is voor de interactie tussen het getij en de morfologie.
We beperken ons tot het vastleggen van het globale gedrag dwz de asymmetrie op het niveau van de hoofdgeul en de hogere niveaus. De getijasymetrie is op lokalere niveaus weliswaar over het algemeen geprononceerder en daarmee makkelijker meetbaar, maar door de overvloed aan lokale bodemveranderingen is ze zonder zeer uitgebreide meetcampagnes nauwelijks te interpreteren.
De parameter zal vastgelegd moeten worden met ADCP- en OSM-metingen.

2. Beschrijving asymmetrie

In een estuarium varieert de eb- en vloedduur. Op de ene lokatie duurt de vloed langer dan de eb en via versa. De relatieve duur van eb en vloed heeft een belangrijke invloed op de snelheden. Omdat bij eb en vloed veelal de zelfde hoeveelheid water door de doorsnede van een estuarium stroomt, leidt een kortere vloedduur tot hogere vloed-snelheden en lagere ebsnelheden en visa versa. Ook heeft de asymmetrie invloed op de duur van de laag- en hoogwaterkentering. Deze verschijnselen, die zich ook op kleinere schaal dan de estuariumdoorsnede voordoen, worden aangeduid met getijasymetrie. Voor een formele beschrijving van het begrip asymmetrie wordt verwezen naar bijlage 1.

Vestiging Middelburg
Postbus 8039, 4330 EA Middelburg
Bezoekadres Grenadierweg 31

Telefoon (0118) 67 22 00
Telefax (0118) 61 65 00

3. Werking van de asymmetrie
De asymmetrie van het horizontale getij levert een bijdrage aan de residuele sedimentbeweging in een estuarium. We maken daarbij een onderscheid tussen relatief grove en fijne sedimenten. De bijdrage voor grof sediment ontstaat doordat er tijdens de kortere periode met hoge snelheden meer sediment getransporteerd wordt dan tijdens de langere periode met lage snelheden. Bij fijn sediment ontstaat de bijdrage o.a. door een verschil in kenteringsduur. Bij fijn sediment leidt dit tot een verschil in transportafstand met eb- en vloed.
Getijasymetrie leidt voor grof sediment tot een resulterend bodemtransport in de richting van de hoogste snelheid. Voor fijn sediment ligt dit gecompliceerder. De kwantitatieve bijdrage die de asymmetrie levert aan de getijgemiddelde transporten van fijn sediment een estuarium, is niet direct aan te geven. Wel is zichtbaar te maken dat getijasymetrie ook voor fijn sediment een essentieel fenomeen is. Het transport van fijn sediment vindt voornamelijk in suspensie plaats.

4. Opbouw van de asymmetrie
Om meer inzicht te krijgen in de werking van de getijasymetrie kan het getij beschouwd worden als de som van een aantal individuele getijcomponenten met als hoofdcomponent het tweemaal daagse maansgetij M2 en als nevencomponenten de residuele stroomsnelheid M0, de viermaaldaagse getijcomponent M4 en de zesmaaldaagse component M6. Figuur 1 en 2 van bijlage 1 laten zien dat de asymmetrie in het getij afhankelijk is van de component (M4 of M6) en van de faseverschillen tussen de componenten. Het complicerende daarbij is dat de M4- en M6-componenten o.a. gegenereerd worden door de interactie van het M2-getij met zijn omgeving.

Vd Kreeke en Rabaczewska (bijlage 1) hebben op basis van de getijcomponenten de interactie geanalyseerd tussen het bodemtransport (grof sediment) en de asymmetrie van het getij.
Uit het onderzoek weergegeven in de bijlage zijn een aantal interessante conclusies te trekken:
1 - De sedimentatie- en erosiepatronen door bedload worden voornamelijk bepaald door het faseverschil tussen M2-M4 en tussen M4-M6 en door de reststroom
2 - De relatieve bijdrage van de component M0, M4 en M6 aan de sedimentatie en erosie wordt bepaald door de amplitudeverhouding M0/M2, M2/M4 en M2/M6 en niet door de snelheid tot derde, vierde of vijfde macht.
3 - De amplitude van de M2-component tot een of andere macht heeft de functie van algemene schalingsfactor.

De hiervoor gegeven analyse is, zoals al eerder is aangegeven, niet direct van toepassing op de totale sedimentbeweging in de Westerschelde doordat het resulterend (suspensie-)transport van slib en fijn zand in de analyse weggelaten is. Door de relatie van het suspensietransport met het bodemtransport, de kenteringsduur en de algehele waterbeweging is er op theoretische gronden ook een indirecte relatie tussen de getijasymetrie en het suspensietransport in een estuarium aan te tonen.

5. Noodzaak metingen
De verdieping zal invloed hebben op de loopsnelheid, demping, generatie en reflectie van de M2-, M4-, en M6-getijcomponent. De asymmetrie zal daardoor veranderen en daarmee het sedimentatiegedrag van het estuarium. Hieraan dragen alle onderdelen van een morfologisch systeem, zoals het intergetijdegebied, de geulen en Noordzeegetijden bij, zonder dat er overigens iets te zeggen is over de relatieve bijdrage van de onderscheiden onderdelen aan het M0-, M4-, M6- en M2-getij in het estuarium. De informatie is daarmee niet uit de geometrie en het Noordzeegetij af te leiden. De getijasymtrie kan alleen goed vastgelegd worden met metingen.

6. Verwachte veranderingen in de asymmetrie
Op grond van proeven in het SCALDIS-model worden een aantal veranderingen in de asymmetrie van het getij door de verdieping verwacht. In deze paragraaf wordt nagegaan wat de effecten van de verdieping zullen zijn voor grof sediment en of de optredende veranderingen meetbaar zullen zijn. De effecten van de verondieping tgv het storten van baggerspecie blijven buiten beschouwing, omdat de gegevens hierover ontbreken. De gevolgen van het storten kunnen in principe lokaal even groot zijn als de gevolgen van het verdiepen.

Om een idee te krijgen over de meetbaarheid zijn de gevolgen van de verdieping voor de asymmetrie voor een twintigtal lokaties geanalyseerd---zie fig.2. Maar een kwart vertoonde mogelijk meetbare verschillen---zie figuur 3 t/m 7.

Lokatie: Platen van Ossenisse I
Veranderingen: meetbaar
Verschijnselen: Er treden sterke veranderingen in de asymmetrie op door het verminderen van de vloedsnelheid. Het zandtranspoort wordt nog sterker ebgedomineerd.

Lokatie: Platen van Ossenisse II
Veranderingen: meetbaar
Verschijnselen: Er treden sterke veranderingen in de asymmetrie op door het verkorten van de vloedduur. Het zandtranspoort wordt minder sterker ebgedomineerd.

Lokatie: Schaar van Waarde I en III
Veranderingen: mogelijk niet meer meetbaar
Verschijnselen: Er treden geen sterke veranderingen in de asymmetrie op. Alleen de amplitude van het getij neemt toe en daarmee de transporten. De erosie- en sedimentatie patronen blijven lokaal hetzelfde. De erosie en sedimentatie nemen echter toe

Lokatie: Schaar van de Noord II
Veranderingen: mogelijk meetbaar
Verschijnselen: Er treden sterke veranderingen in de asymmetrie op door het verminderen van de vloedsnelheid. Het zandtranspoort wordt minder sterk ebgedomineerd.

De lokaties met mogelijk meetbare verschillen liggen in de directe omgeving van de verdiepingswerken dwz in het oostelijk deel. Uit computerberekeningen blijkt er veranderingen in het getij tot voor de Vlaamse en Walcherse kust optreden. Deze zullen echter niet meetbaar zijn. Omdat alleen de veranderingen in de directe omgeving van de verdieping meetbaar zijn, zouden de metingen tot het oostelijk deel beperkt kunnen blijven. Geadviseerd wordt om dit niet te doen, omdat de stortingen ook effect kunnen hebben en die vinden voornamelijk in het westen plaats.

7. Opzet vd metingen
Voor het meten van de asymmetrie op het niveau van de geul of hoger moeten er zowel debietmetingen als langdurige OSM-metingen uitgevoerd worden.
- Debietmetingen
Voor het vastleggen van de asymmetrie in een meetraai zijn snelheidsmetingen nodig over de volle dwarsdoorsnede van het estuarium. Ivm het bodem en suspensietransport moeten zowel de snelheden zo dicht mogelijk aan de bodem vastgelegd worden als de snelheden hoger in het waterlichaam. Voorlopig wordt voorgesteld om in de standaardraaien ---zie fig. 1 over de volle breedte van het estuarium simultane ADCP-metingen uit te voeren. We missen daarmee de belangrijke onderste 6% van de waterkolom, maar elders krijgen we een veel dichtere bemonstering. De metingen zouden over een periode van liefst 25 uur uitgevoerd moeten worden en wel tijdens springtij, gemiddeldtij en doodtij.

OSM-metingen
Om de debietmetingen voor en na de verdieping te kunnen normeren naar een standaard getij moeten er op een aantal plaatsen in de geuldoorsnede over een periode van minimaal 29 dagen snelheidsregistraties beschikbaar zijn. Gedacht wordt om per geul minimaal 2 metingen uit te voeren ivm de mogelijkheid van lokale eb- en vloeddominantie in een geul.

8. Meetfrequentie
De meetfrequentie is enerzijds afhankelijk van meetbaarheid van de verschillen en anderzijds de snelheid waarmee de maatgevende processen verlopen. We beperken ons hier eerst tot de snelheid waarmee processen verlopen. In een estuarium spelen processen met een verschillende ruimte- en tijdschaal een rol. Deze schalen zijn veelal gekoppeld dwz dat bij een grote ruimteschaal ook een grote tijdschaal hoort.
In tabel 1 is weergeven welke tijdschalen mijns inziens van belang zijn en welke ruimteschalen daarbij horen. Een natuurlijk systeem zal in dit concept wanneer het uit evenwicht gebracht wordt en daarna vrij wordt

gelaten met de tijdschaal van De maatgevende processen (kolom 1) terugkeren naar evenwicht. In de waterbeweging (asymmetrie) zien we dan ook in dit tempo veranderingen optreden.
Het heeft dan bij een natuurlijk systeem geen zin om verschijnselen met een tijdschaal van 50j of meer te monitoren met een tijdsinterval van minder dan 5j. Dit ligt anders als het systeem volledig geforceerd wordt met baggerwerken. Dan is de tijdschaal en ruimteschaal van de baggerwerken kolom 2 maatgevend. Voor de verdieping resulteert dit in de meetintervallen van kolom 3.

RUIMTESCHAAL	TIJDSCHAAL natuur	TIJDSCHAAL met baggeren	MEETINTERVAL bij baggeren	MEETINTERVAL ivm nauwkeu.
Hele estuarium	orde 1000j	orde 1000j	100j	5j.
Eb/vloedgeulpaar	orde 50j	orde 10j	1j	2j.
Geul	orde 5j	orde 5j	.5j	1j.
Drempel	orde 5j	orde 2j	.2j	1j.
Geul/plaatpaar	orde .5j	orde .5j	.1j	-

Tabel 1. Schalen en meetintervallen.

Voorgesteld wordt ivm de nauwkeurigheid de metingen 1x per 2 jaar uit te voeren.

9. Verwerking
Op de ADCP-metingen moeten de volgende bewerkingen worden:
- Herleiden van de metingen naar een dwarsprofiel-gemiddelde snelheid Vg.
- Harmonische analyse op M0, M2, M4 en M6 van Vg.

Op de snelheden Vp van de puntmetingen (OSM-metingen) moeten de volgende bewerkingen uitgevoerd worden:
- Harmonische analyse op M0, M2, M4 en M6 van Vp.
- Koppeling van de analyse van Vp aan de analyse van Vg

NB. Dit meetprogramma is nog niet uitgekristalliseerd. Het ligt in de bedoeling een aantal deskundigen te raadplegen om met meetprogramma aan te scherpen. Verder moet nagegaan worden in hoeverre de bestaande metingen in het kader van "kortsluitgeulen", OOSTWEST en "drempel" bruikbaar zijn als T0 en om het programma aan te scherpen.

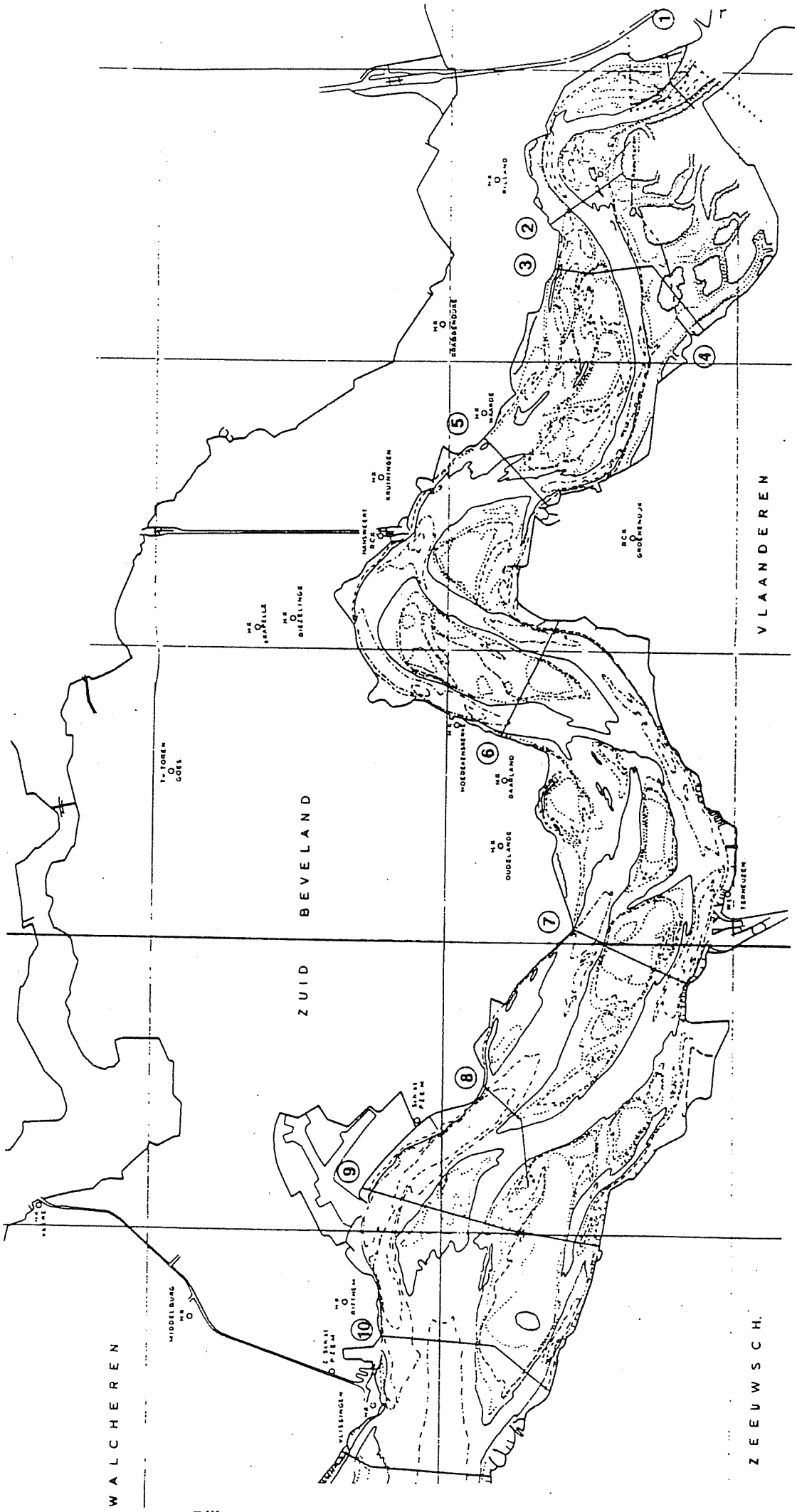

Bijlage 1: Overzicht van de ligging van de debietraaien in de Westerschelde.

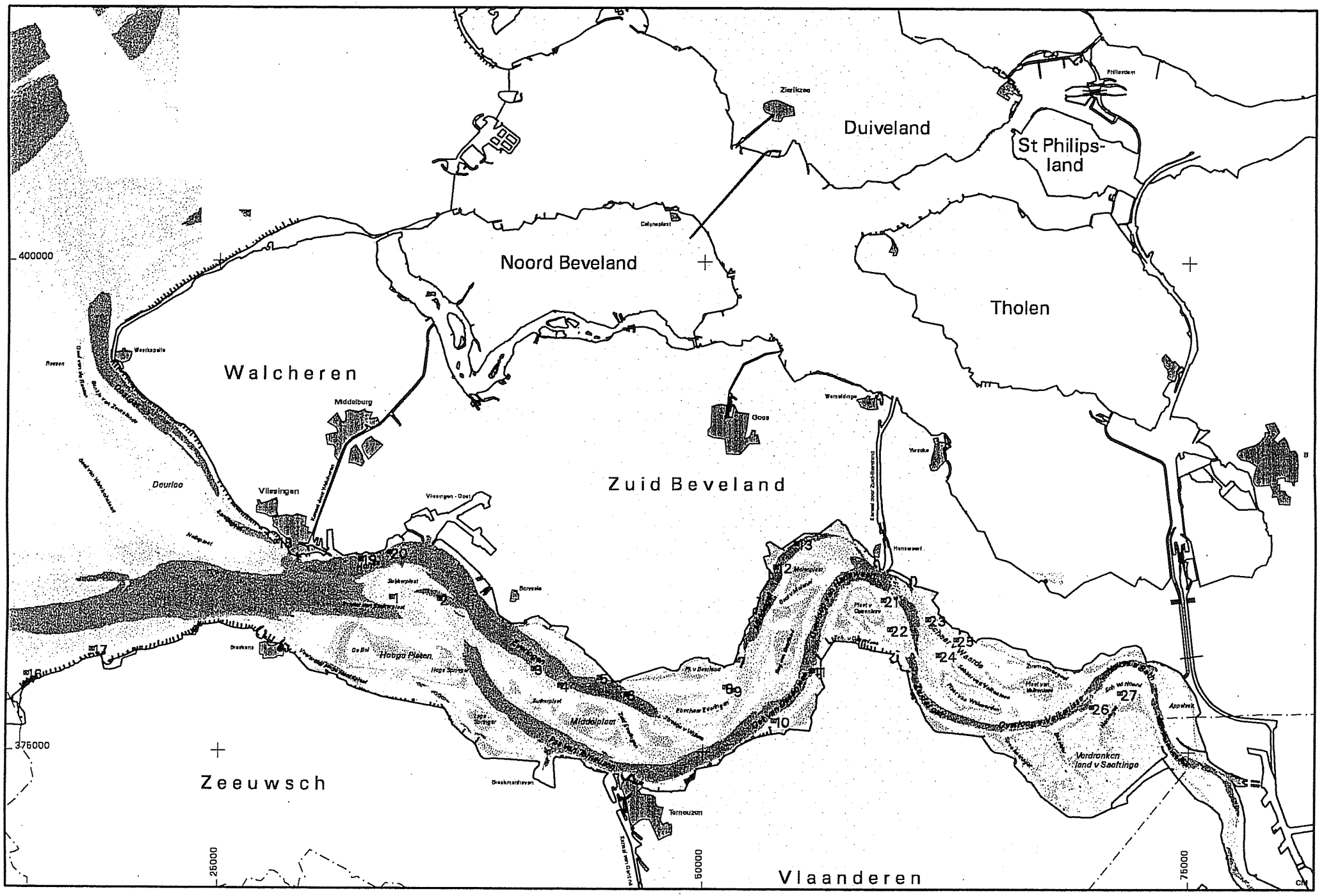
Duiveland
St Philips-
land
Noord Beveland
Tholen
Walcheren
Zuid Beveland
Zeeuwsch
Vlaanderen
Middelburg
Vlissingen
Goes
Zierikzee
Deurloo
Hoboa Platen
Middelplaat
Vordronken
land v Saaftinge
400000
375000
25000
50000
75000

Scaldis model, gemtij zonder verdieping
Scaldis model, gemtij zonder verdieping
Scaldis model, gemtij met verdieping
Scaldis model, gemtij met verdieping

IDP: 97/03/24 16:02:27 SIM: 97/03/24 16:02
IDP: 97/03/24 16:02:27 SIM: 97/03/24 16:02
IDP: 97/03/24 16:05:30 SIM: 97/03/24 16:05
IDP: 97/03/24 16:05:30 SIM: 97/03/24 16:05

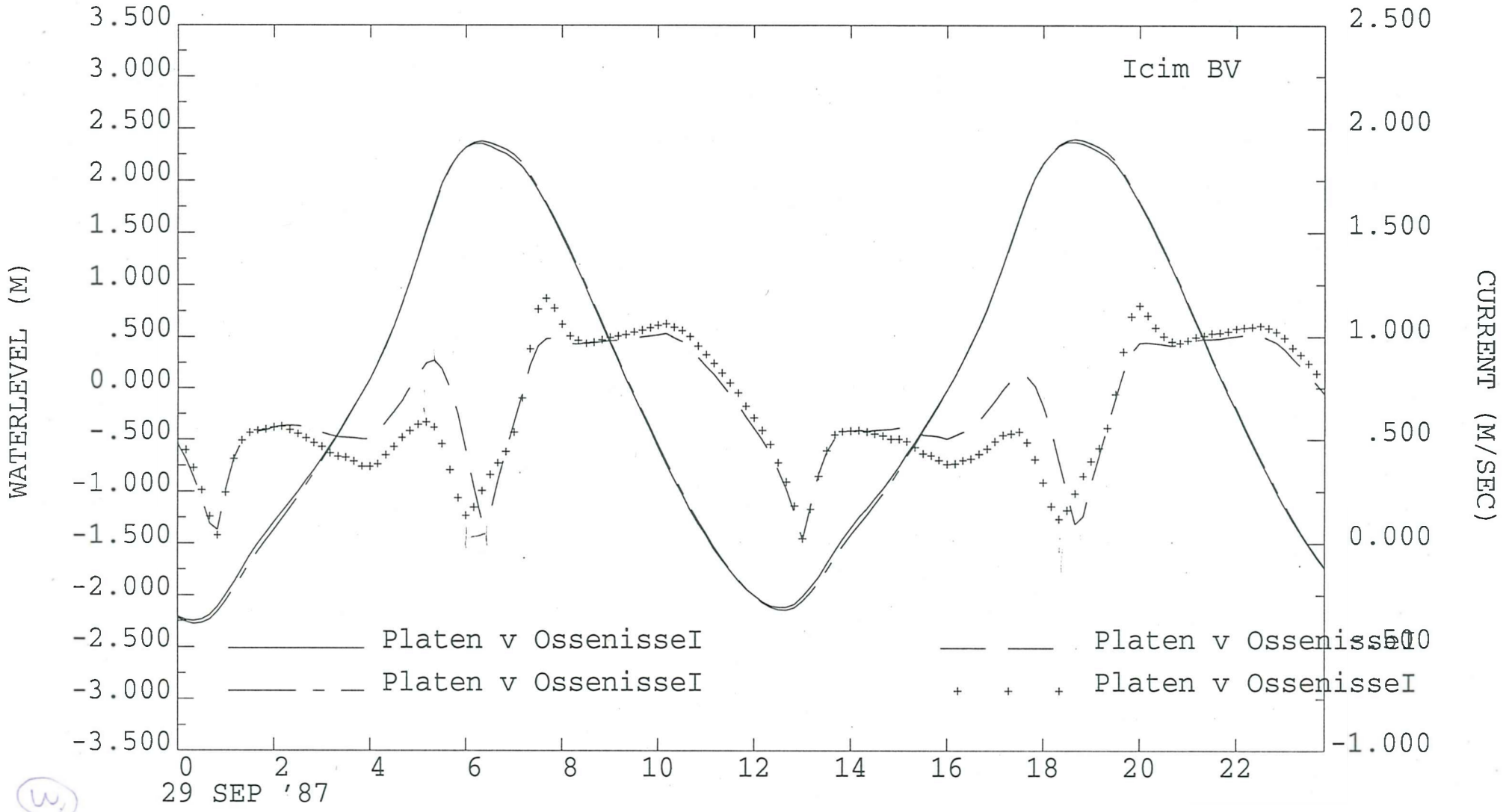

COMPUTED WATERLEVEL AT STATION
COMPUTED CURRENT AT STATION
COMPUTED WATERLEVEL AT STATION
COMPUTED CURRENT AT STATION

Scaldis model, gemtij zonder verdieping
Scaldis model, gemtij zonder verdieping
Scaldis model, gemtij met verdieping
Scaldis model, gemtij met verdieping

IDP: 97/03/24 16:02:27 SIM: 97/03/24 16:02
IDP: 97/03/24 16:02:27 SIM: 97/03/24 16:02
IDP: 97/03/24 16:05:30 SIM: 97/03/24 16:05
IDP: 97/03/24 16:05:30 SIM: 97/03/24 16:05

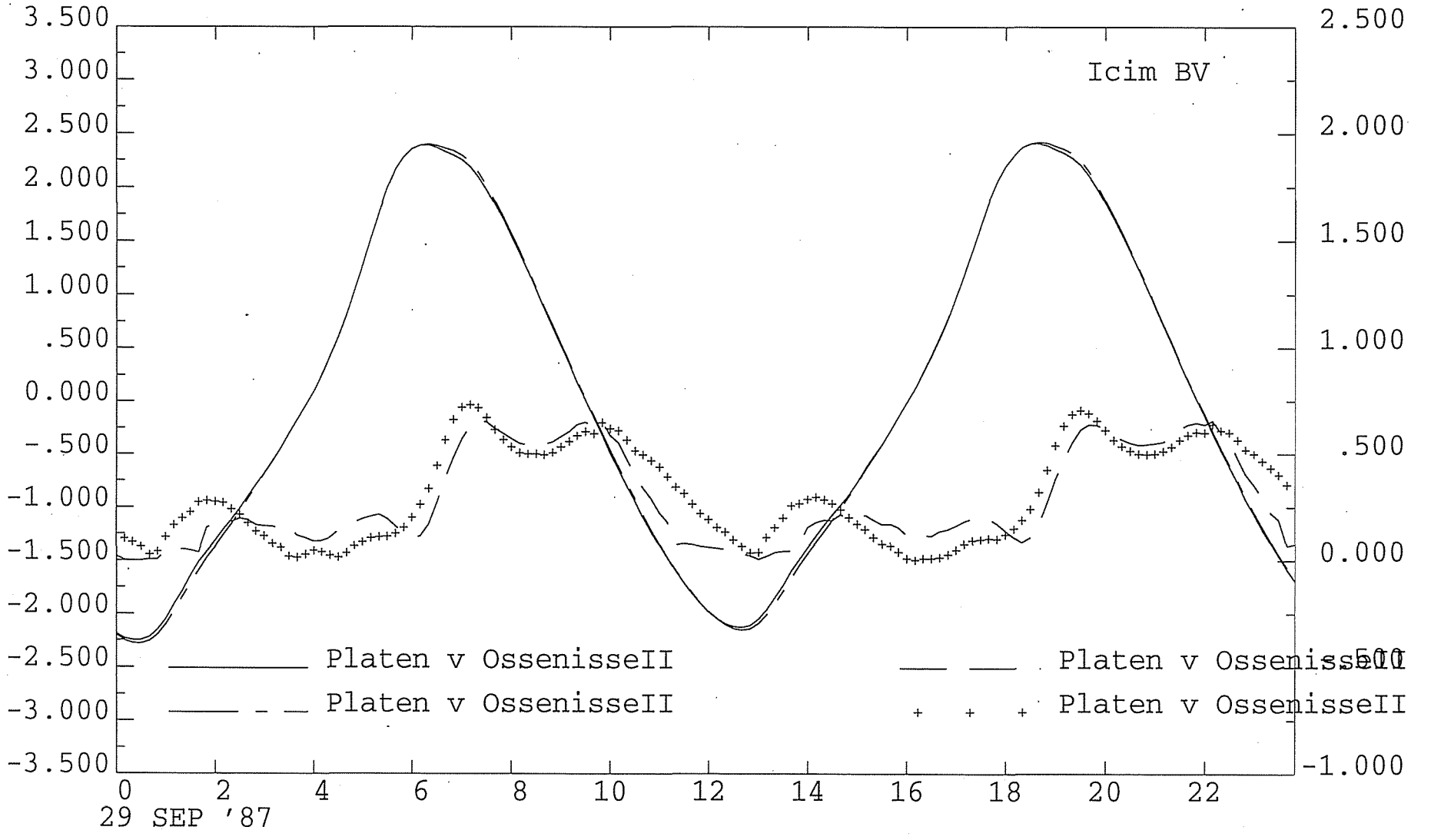

COMPUTED WATERLEVEL AT STATION
COMPUTED CURRENT AT STATION
COMPUTED WATERLEVEL AT STATION
COMPUTED CURRENT AT STATION

PLOT 10

Scaldis model, gemtij zonder verdieping
Scaldis model, gemtij zonder verdieping
Scaldis model, gemtij met verdieping
Scaldis model, gemtij met verdieping

IDP: 97/03/24 16:02:27 SIM: 97/03/24 16:02
IDP: 97/03/24 16:02:27 SIM: 97/03/24 16:02
IDP: 97/03/24 16:05:30 SIM: 97/03/24 16:05
IDP: 97/03/24 16:05:30 SIM: 97/03/24 16:05

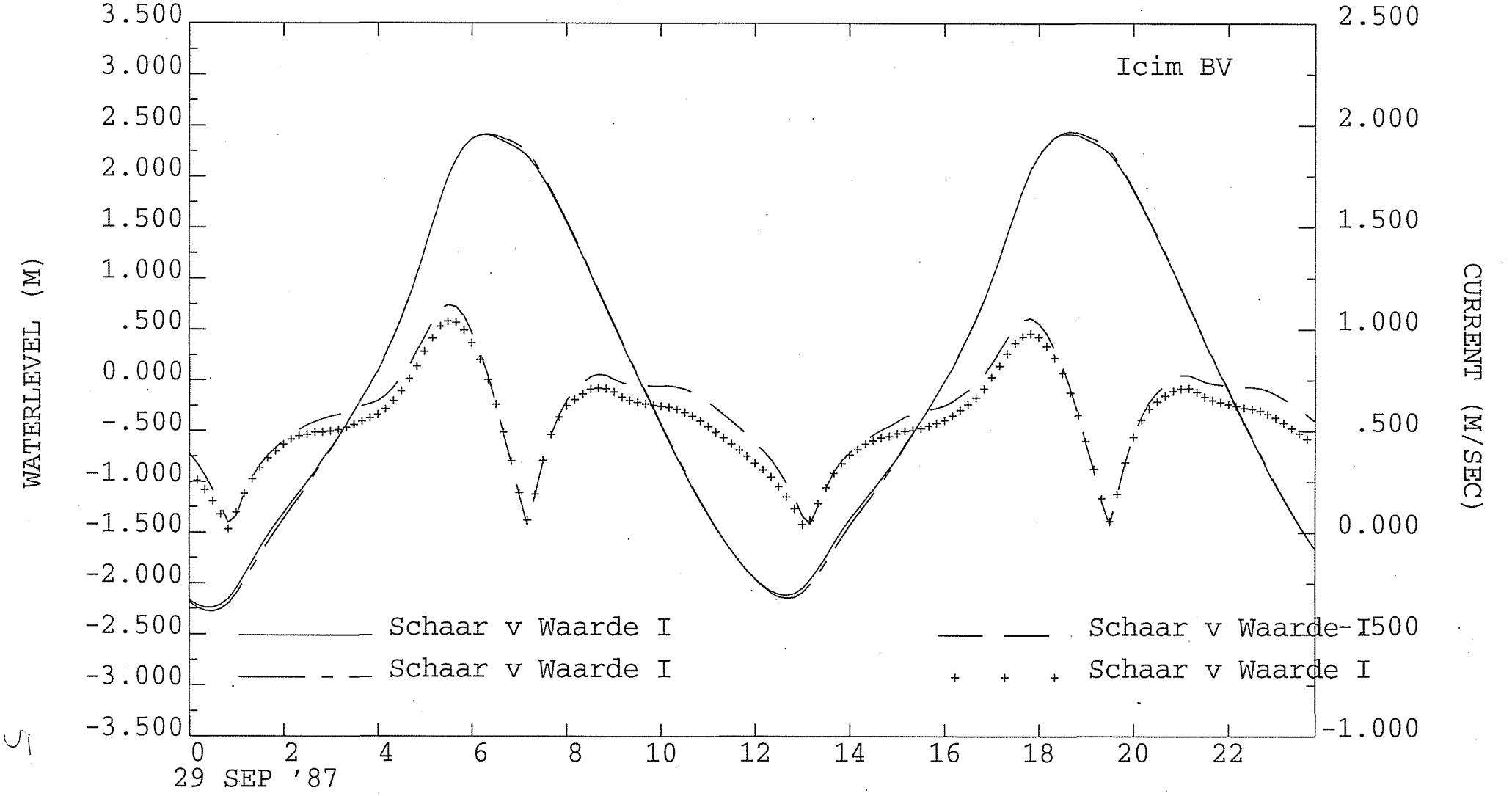

51

PLOT 11

Scaldis model, gemtij zonder verdieping
Scaldis model, gemtij zonder verdieping
Scaldis model, gemtij met verdieping
Scaldis model, gemtij met verdieping

IDP: 97/03/24 16:02:27 SIM: 97/03/24 16:02
IDP: 97/03/24 16:02:27 SIM: 97/03/24 16:02
IDP: 97/03/24 16:05:30 SIM: 97/03/24 16:05
IDP: 97/03/24 16:05:30 SIM: 97/03/24 16:05

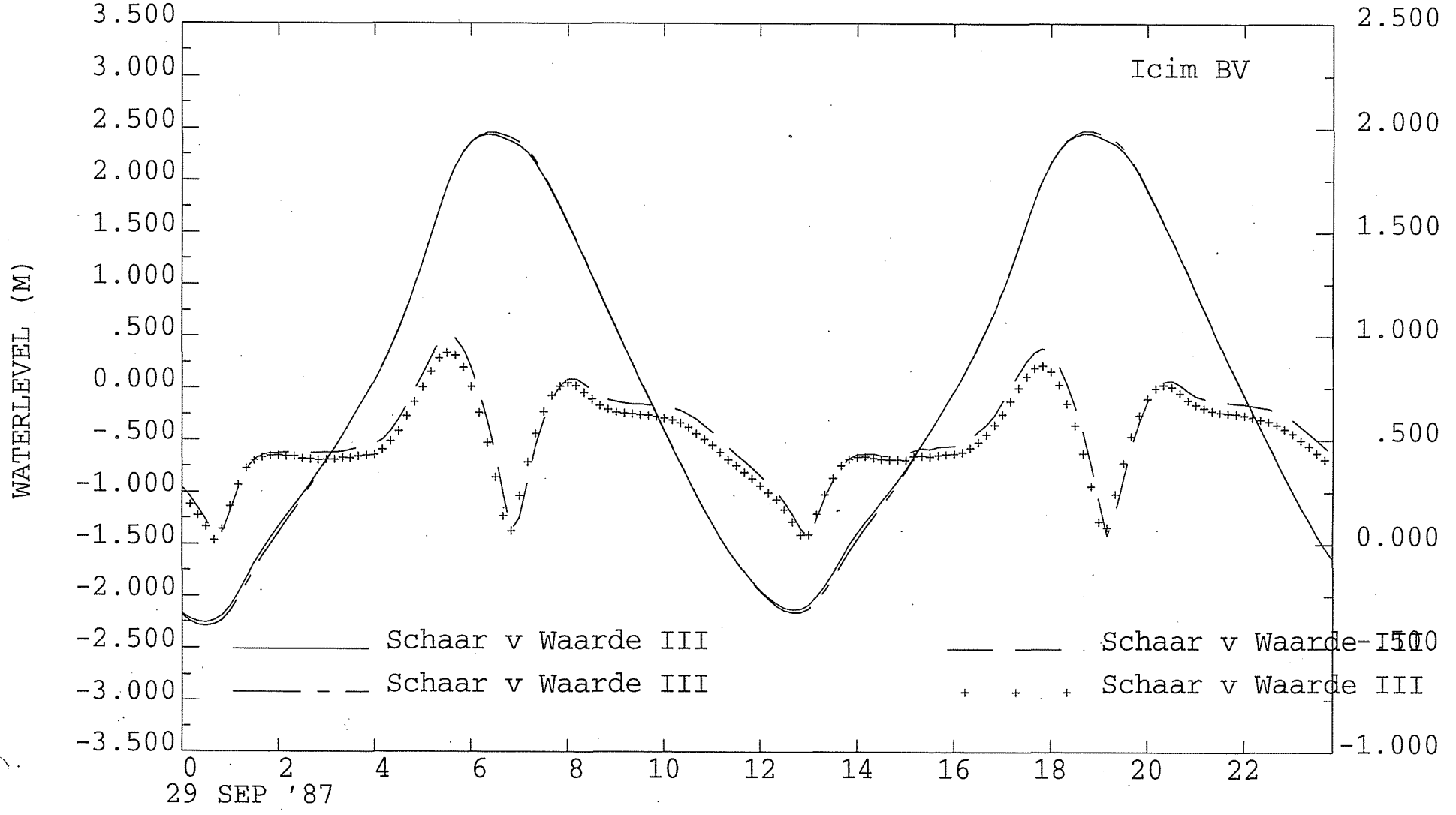

COMPUTED WATERLEVEL AT STATION
COMPUTED CURRENT AT STATION
COMPUTED WATERLEVEL AT STATION
COMPUTED CURRENT AT STATION

PLOT 1

Scaldis model, gemtij zonder verdieping
Scaldis model, gemtij zonder verdieping
Scaldis model, gemtij met verdieping
Scaldis model, gemtij met verdieping

IDP: 97/03/24 16:02:27 SIM: 97/03/24 16:02
IDP: 97/03/24 16:02:27 SIM: 97/03/24 16:02
IDP: 97/03/24 16:05:30 SIM: 97/03/24 16:05
IDP: 97/03/24 16:05:30 SIM: 97/03/24 16:05

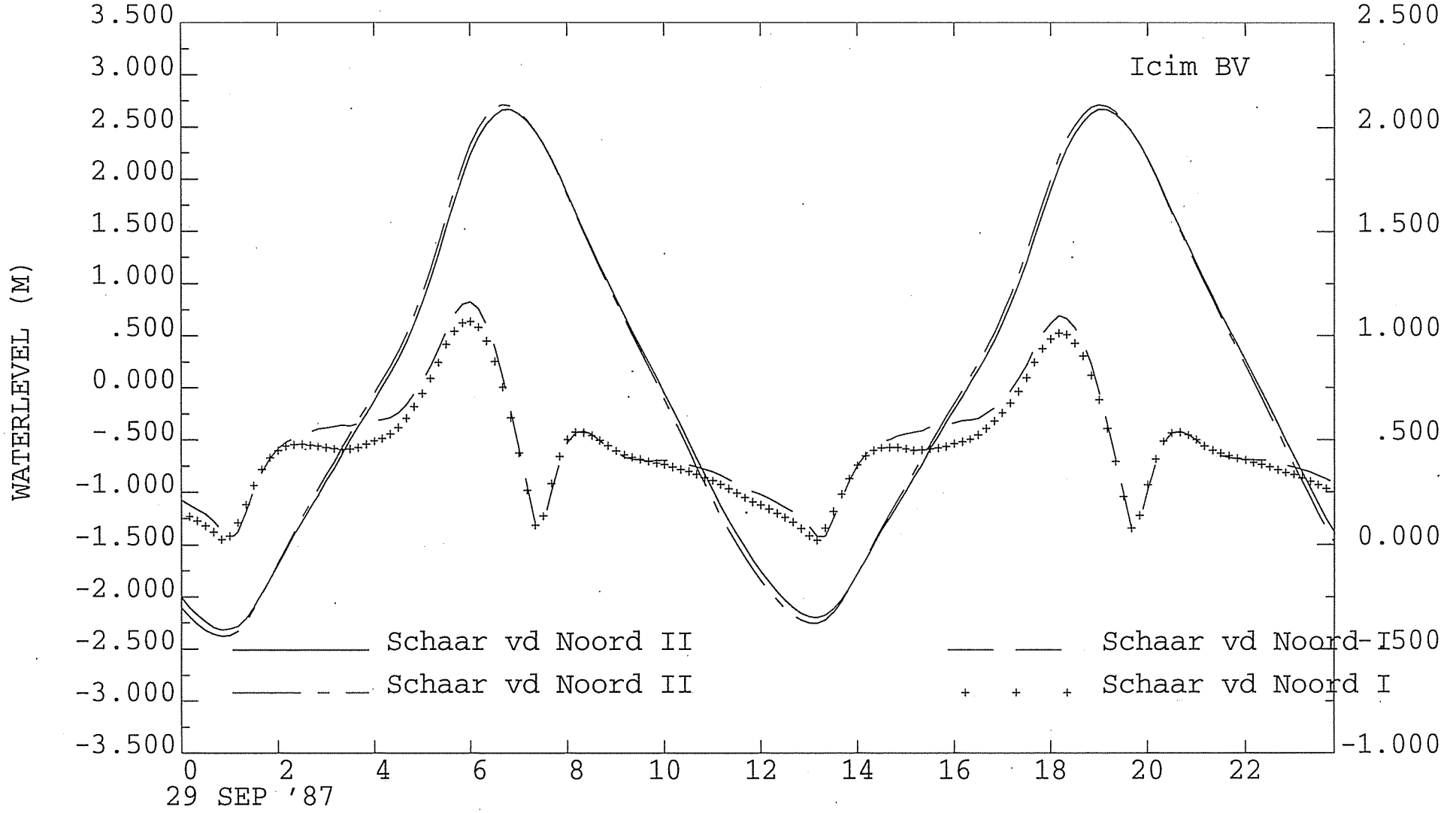

COMPUTED WATERLEVEL AT STATION
COMPUTED CURRENT AT STATION
COMPUTED WATERLEVEL AT STATION
COMPUTED CURRENT AT STATION

PLOT 3

BYLAGE 1

Netherlands Journal of Sea Research
31 (3): 209-220 (1993)

TIDE-INDUCED RESIDUAL TRANSPORT OF COARSE SEDIMENT; APPLICATION TO THE EMS ESTUARY

J. VAN DE KREEKE[1] and K. ROBACZEWSKA[2]

[1]*Rosenstiel School of Marine and Atmospheric Science, University of Miami, 4600 Rickenbacker Causeway Miami, Fla 33149 USA*
[2]*Ministry of Transport, Public Works and Water Management, Directorate-General for Public Works and Water Management Tidal Waters Division, Koningskade 4, 2500 EX The Hague, the Netherlands*

ABSTRACT

For a tidal channel with water of homogeneous density, an approximate analytical expression is derived for the tidally averaged transport of coarse sediment in terms of the amplitudes and phases of the tidal-current constituents. Transport is in the form of bed load and the rate of transport is proportional to some power of the local current speed. It is assumed that the tidal current is dominated by the M_2 constituent. From the analytical expression it follows that the interactions of M_2 and M_0 (= Eulerian mean current) and of M_2 and any of its even overtides, M_4, M_8 *etc.*, constitute the major contribution to the tidally averaged sediment transport. A combination of the M_2 tidal current and a fundamental constituent in the diurnal, semidiurnal or subsequent period bands results in a tidally averaged transport that fluctuates with the corresponding beat frequency. Therefore, for the long-term mean bed-load transport only the contributions of M_2 and M_0 and of M_2 and its even overtides are of interest. Application to the main channel of the Ems estuary showed good agreement with transport pathways derived from the grain-size distribution pattern. The tidally averaged sediment transport is largely the result of the interaction of the M_2 and M_0 tidal current constituents.

1. INTRODUCTION

In the literature considerable attention has been given to the effect of tidal-current asymmetry on the transport of coarse sediment (*e.g.* PINGREE & GRIFFITH, 1979; BOON & BYRNE, 1981; DRONKERS, 1986; AUBREY, 1986; FRIEDRICHS & AUBREY, 1988; FRY & AUBREY, 1990). In particular these studies focus on the tidally averaged sediment transport as a result of the asymmetry introduced by the interaction of M_2 and M_4. Here a more general approach is taken and the effect of the interaction of all tide constituents, including the residual current, on the coarse-sediment transport is investigated. In the analysis, it is assumed that M_2 is the dominant tidal-current constituent and that all other constituents are of a lesser order of magnitude. This condition is reasonably satisfied in most estuaries in the Netherlands.

To show the contribution of the various constituents, an approximate analytical expression for the tidally averaged sediment transport was developed. The expression was used to calculate the long-term mean sediment transport for a large number of stations in the Ems estuary. Application of the analytical expression requires knowledge of the various tidal-current constituents. This information was obtained from one-month-long time series of currents generated in a two-dimensional vertically-integrated model for the hydrodynamics of the estuary (ROBACZEWSKA *et al.*, 1992). The long-term averaged coarse-sediment transport pattern calculated with the analytical expression is compared with the transport pattern derived from spatial variations in the grain-size distribution (MCLAREN, 1991).

2. TIDAL-CURRENT ASYMMETRY

In the literature tidal-current asymmetry is used somewhat loosely and is meant to imply that the flood part of the velocity-time curve has a shape different from the part representing the ebb. For purposes of this discussion a rather stricter definition of (a-)symmetry is introduced that corresponds to the concept of (a-)symmetry in mathematics. Consider a rectilinear current $u(t)$ that is periodic with zero mean. Defining a symmetry axis at the time of slack water, $t=t_0$, the curve $u(t)$ is symmetric about $t=t_0$ when

$$|u(t_0+t)| = |u(t_0-t)| \qquad \text{(eq. 1)}$$

The absolute value $|u|$ represents the current speed.

When considering a single fundamental harmonic,

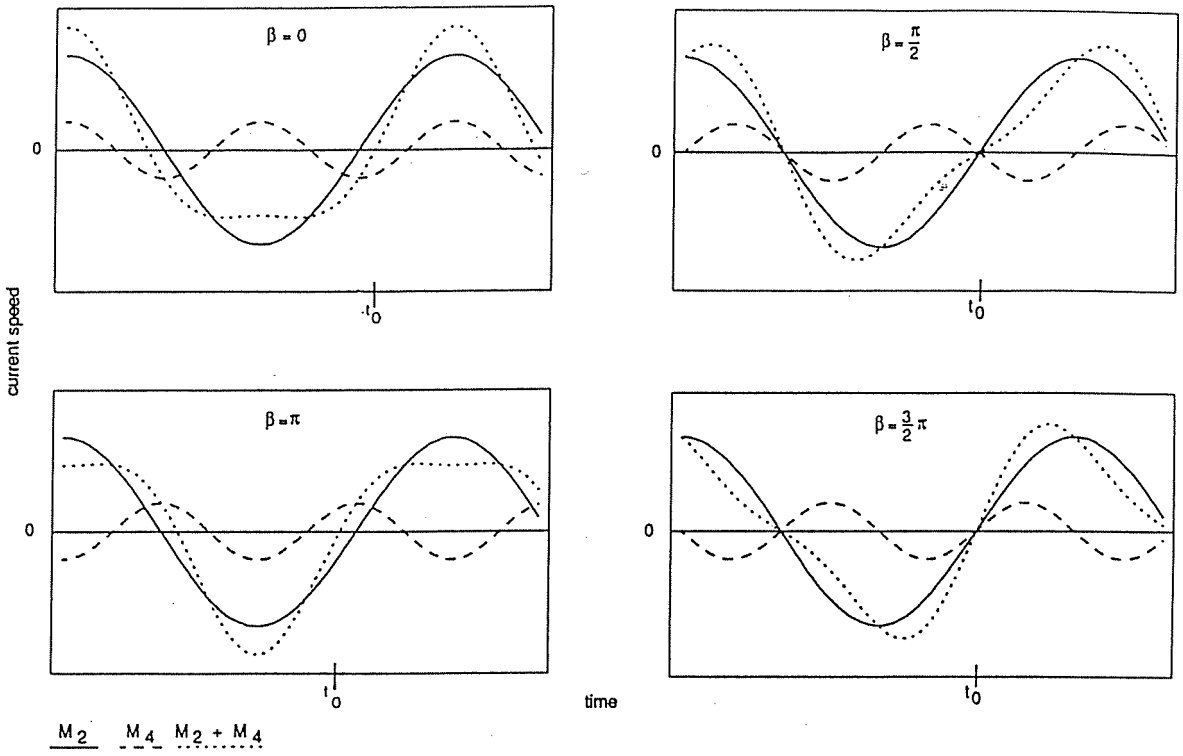

Fig. 1. M_2 and M_4 tidal-current constituents.

e.g. M_2, the asymmetry in the velocity curve is a result of the presence of overtides. For M_2 and its first overtide M_4, and assuming a rectilinear current, the velocity can be expressed as

$$u(t) = \hat{u} \cos \sigma t + \hat{u}_4 \cos (2\sigma t - \beta) \qquad \text{(eq. 2)}$$

in which $\hat{u}$ is the amplitude of the M_2 tidal current, $\hat{u}_4$ is the amplitude of the M_4 tidal current, σ is the angular frequency of the M_2 tide and β is the phase of M_4 relative to M_2. Substituting in Eq. (1) it can be shown that the curve $u(t)$ is symmetric only for $\beta=\pi/2$ and $\beta=3\pi/2$. For all other values, the velocity is asymmetric. For $-\pi/2 < \beta < \pi/2$ flood velocities (defined as positive) are larger and flood duration is shorter than for the ebb. The reverse holds for $\pi/2 < \beta < 3\pi/2$. This is illustrated in Fig. 1.

For a combination of the M_2 and M_6 tidal-current constituents, the velocity curve is

$$u(t) = \hat{u} \cos \sigma t + \hat{u}_6 \cos (3\sigma t - \gamma) \qquad \text{(eq. 3)}$$

Here, $\hat{u}_6$ is the amplitude of the M_6 tidal current and γ is the phase angle of the M_6 tidal current relative to the M_2 tidal current. Substituting in Eq. (1) it can be shown that the velocity curve is symmetric only for $\gamma=0$ and $\gamma=\pi$. This is illustrated in Fig. 2. In general then, the velocity curve for a combination of the M_2 tidal current and any of its overtides is asymmetric!

For future reference, a property of the combination of the M_2 tidal current and its odd overtides is pointed out, *viz.*,

$$u(t) = - u (t + T/2) \qquad \text{(eq. 4)}$$

The current speed is periodic with a period $T/2$, where T is the period for the M_2 tide. For this see also Fig. 2.

Contrary to FRY & AUBREY (1990), we make no attempt to relate tidal water-level asymmetry and tidal-current asymmetry.

3. TIDAL-CURRENT ASYMMETRY AND COARSE-SEDIMENT TRANSPORT

To determine the effect of the tidal variations in the current on the transport of coarse sediment, the following transport model is introduced. Coarse sediment is defined as having a diameter such that $u_*/w<1$, where u_* is the shear velocity and w is the fall velocity. The sediment is transported as bed load (BAGNOLD, 1966). Furthermore it is assumed that the rate of the bed-load transport is a function of the local velocity *viz.*,

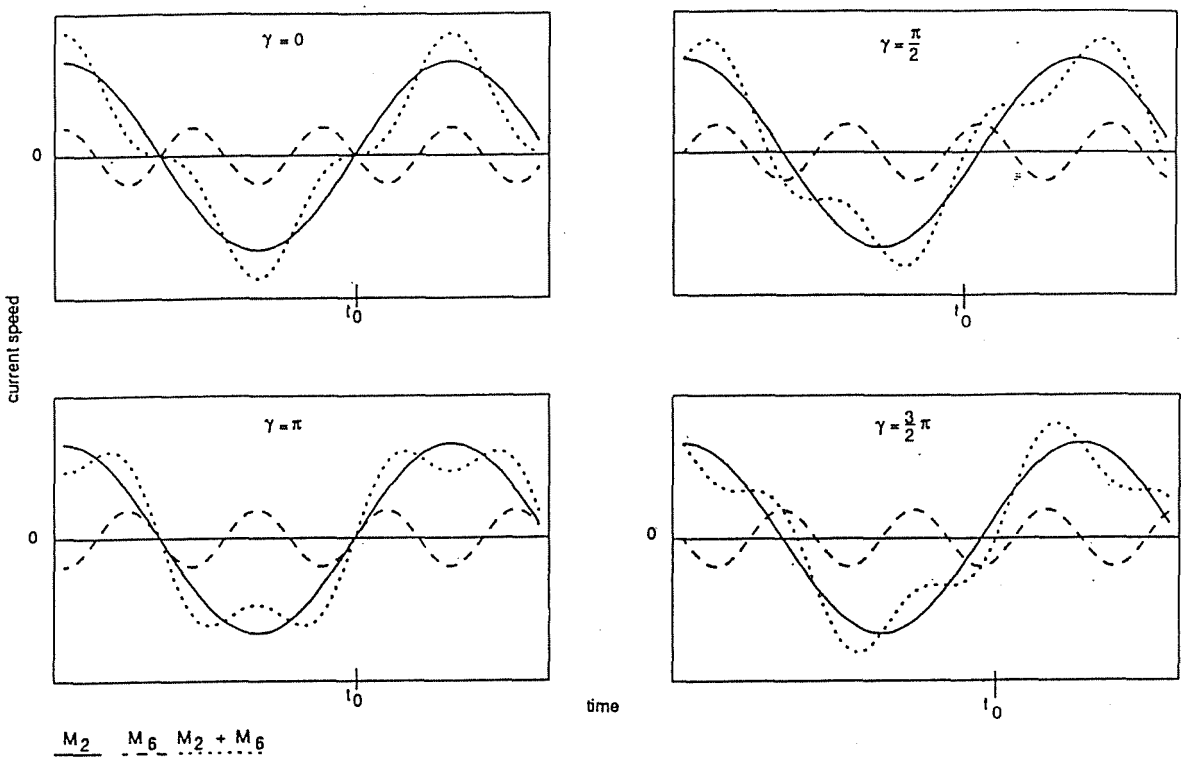

Fig. 2. M_2 and M_6 tidal-current constituents.

$$q = f|u|^n \operatorname{sign} u \qquad \text{(eq. 5)}$$

where
q = volumetric rate of sediment transport per unit width
f = function of sediment - and fluid characteristics
u = depth-averaged velocity
n = a number varying between 3 and 5

As an example, when taking the formula developed by BAGNOLD (1966) and the value of n=3, the expression for the function f is

$$f = \frac{\rho}{(\rho_s - \rho)\, g\, (\tan\phi - \tan\theta)} \frac{e_b}{F} \qquad \text{(eq. 6)}$$

where
ρ = density of water
ρ_s = density of sediment
e_b = efficiency factor (≈0.1)
ϕ = angle of repose of bed material (tan ϕ≈0.6)
θ = local bed slope
F = friction factor

In discussing net bed-load transport previous studies (*e.g.* PINGREE & GRIFFITH, 1979; AUBREY, 1986 and FRY & AUBREY, 1990) have concentrated on tidal asymmetry associated with M_2 and a single overtide, M_4. For the combination of M_2 and M_4 the velocity u is given by Eq. (2). Substituting for u in Eq. (5) and taking into account the difference in shape of the velocity curve for different values of the phase angle β (see Fig. 1), it follows that for $-\pi/2 < \beta < \pi/2$ the tidally averaged bed-load transport is in the flood (positive) direction and for $\pi/2 < \beta < 3\pi/2$ it is in the ebb direction. For $\beta=\pi/2$ and $\beta=3\pi/2$, the tidally averaged sediment transport is zero. For a tidal-current field consisting only of an M_2 and M_4 constituent, the value of the phase angle β determines the direction of the tidally averaged bed-load transport. This was demonstrated earlier by AUBREY (1986), who numerically calculated the flood-to-ebb ratio of the bed-load transport for different values of the phase angle β. In his calculations he assumed a bed-load transport formula similar to Eq. (5) with n=3.

For a tidal current consisting of the constituents M_2 and M_6, the velocity curve is given by Eq. (3). Substituting for u in Eq. (5) and making use of the property of the velocity curve expressed by Eq. (4), it follows that the tidally averaged bed-load transport is zero for all values of the phase angle γ. Obviously, tidal asymmetry does not guarantee a net bed-load transport.

The foregoing qualitative discussion focuses on M_2

and its first even (M_4) and first odd (M_6) overtide. It can be easily verified that the conclusions arrived at with regard to the tidally averaged sediment transport for M_2 and M_4 hold for any combination of M_2 and one of its higher even overtides (M_8, M_{12}....). Also for a combination of M_2 and any of its higher odd overtides (M_{10}, M_{14}...), the tidally averaged bed-load transport is always zero. Whereas the foregoing is restricted to a combination of M_2 and a single overtide, in the following the effect on the tidally averaged bed-load transport of a combination of M_2 and several overtides, other fundamental harmonics and a tidal mean current is investigated. For this an approximate analytical expression for the tidally averaged bed-load transport is derived.

4. APPROXIMATE EXPRESSION FOR THE TIDALLY AVERAGED TRANSPORT OF COARSE SEDIMENT

Approximate expressions for the tidally averaged bed-load transport are presented that include the following sets of tidal current constituents
-M_2, M_0, M_4, M_6, S_2
-M_2, M_0, M_4, M_6, S_2, N_2, MS_4, K_1.

In the following, for the first set of tidal-current constituents a step-by-step derivation of the approximate expression is given. For the second set of tidal-current constituents the final result is presented in Appendix A. In deriving the approximate analytical expressions it is assumed that the velocity field is dominated by the M_2 tidal-current constituent, *i.e.* the amplitude of M_2 is an order of magnitude larger than the amplitudes of the other fundamental tidal constituents and overtides and the magnitude of the Eulerian mean current M_0. This condition is reasonably satisfied in the Dutch estuaries. As an example see Fig. 5. For the first set of tidal-current constituents the rectilinear velocity field is expressed as

$$u(t) = \hat{u}\cos\sigma t + \hat{u}_4\cos(2\sigma t-\beta) + \hat{u}_6\cos(3\sigma t-\gamma) + u_0 + \hat{u}_2\cos(\sigma_1 t-\alpha_1) \qquad \text{(eq. 7)}$$

in which

$\hat{u}$ = amplitude of the M_2 tidal current
$\hat{u}_4$ = amplitude of the M_4 tidal current
$\hat{u}_6$ = amplitude of the M_6 tidal current
$\hat{u}_2$ = amplitude of the S_2 tidal current
u_o = Eulerian residual velocity
σ = angular frequency of the M_2 tidal current
σ_1 = angular frequency of the S_2 tidal current
α_1 = phase of the tidal current S_2 relative to the M_2 tidal current
β = phase of the tidal current M_4 relative to the M_2 tidal current
γ = phase of the tidal current M_6 relative to the M_2 tidal current

Normalizing the expression for $u(t)$ by the amplitude of M_2 results in

$$\frac{u(t)}{\hat{u}} = \cos\sigma t + \varepsilon_4\cos(2\sigma t-\beta) + \varepsilon_6\cos(3\sigma t-\gamma) + \varepsilon_0 + \varepsilon_2\cos(\sigma_1-\alpha_1) \qquad \text{(eq. 8)}$$

where

$$\varepsilon_4 = \frac{\hat{u}_4}{\hat{u}}, \quad \varepsilon_6 = \frac{\hat{u}_6}{\hat{u}}, \quad \varepsilon_0 = \frac{u_0}{\hat{u}}, \quad \varepsilon_2 = \frac{\hat{u}_2}{\hat{u}}$$

and

$\varepsilon_4 \ll 1$, $\varepsilon_6 \ll 1$ $\varepsilon_0 \ll 1$, $\varepsilon_2 \ll 1$

Introducing $\sigma_1 = \sigma + \Delta\sigma$ the expression for $u/\hat{u}$ is

$$\frac{u(t)}{\hat{u}} = \cos\sigma t(1+\varepsilon_2\cos(\Delta\sigma t-\alpha_1)) - \varepsilon_2\sin(\Delta\sigma t-\alpha_1)\sin\sigma t + \varepsilon_4\cos(2\sigma t-\beta) + \varepsilon_6\cos(3\sigma t-\gamma) + \varepsilon_0 \qquad \text{(eq. 9)}$$

Here $\Delta\sigma$ is the beat frequency of M_2 and S_2. Using Eq. 5 with n=3 as the relation between sediment transport and velocity field and substituting for u(t) from Eq. (9) results in the following expression for the dimensionless tidally averaged bed-load transport.

$$\frac{\langle q\rangle}{f\hat{u}^3} = \langle[(1+\varepsilon_2\cos(\Delta\sigma t-\alpha_1))\cos\sigma t - \varepsilon_2\sin(\Delta\sigma t-\alpha_1)\sin\sigma t + \varepsilon_4\cos(2\sigma t-\beta) - \varepsilon_6\cos((3\sigma t-\gamma)+\varepsilon_0)]^3\rangle \qquad \text{(eq. 10)}$$

where the angle brackets stand for the operation

$$\langle\ \rangle = \frac{1}{T}\int_{t_1-T/2}^{t_1+T/2} dt \qquad \text{(eq. 11)}$$

in which T is the period of the M_2 constituent. When neglecting terms of $0(\varepsilon^3)$ and higher the result is

$$\frac{\langle q\rangle}{\hat{u}^3 f} = \frac{3}{2}\varepsilon_0 \qquad M_2, M_0$$

$$+\frac{3}{4}\varepsilon_4\cos\beta \qquad M_2, M_4$$

$$+\frac{3}{2}\varepsilon_4\varepsilon_6\cos(\beta-\gamma) \qquad M_2, M_4, M_6$$

$$+ \frac{3}{2}\varepsilon_4 \varepsilon_2 \cos(\Delta\sigma t_1 + \beta) \qquad M_2, M_4, S_2$$

$$+ 3\varepsilon_2 \varepsilon_0 \cos(\Delta\sigma t_1 - \alpha_1) \qquad M_2, M_0, S_2$$

(eq. 12)

In this equation, each term is the result of the interaction of two or more tidal constituents written behind it. The interactions of M_2 and M_0, M_2 and M_4 and the triple interactions M_2, M_4 and M_6 lead to a constant net flux of sediment. Interactions that involve S_2 cause a sediment flux that varies in time with the beat frequency $\Delta\sigma$. This frequency corresponds to a period of about 14 days. Therefore, the long-term (several months) tide-induced bed-load flux is given by the first three terms in Eq. (12),

$$\frac{\langle q \rangle}{\hat{u}^3 f} = \frac{3}{2}\varepsilon_0 + \frac{3}{4}\varepsilon_4 \cos\beta + \frac{3}{2}\varepsilon_4\varepsilon_6 \cos(\beta - \gamma)$$

(eq. 13)

In agreement with what is stated in Chapter 3, the direction and magnitude of the contribution of the interaction of M_2 and M_4 to the sediment flux are determined by the phase angle β. Also, in agreement with Chapter 3, there is no contribution to the net flux by the interaction of M_2 and M_6. However, there is a second-order contribution to the net sediment flux by the triple interaction between M_2, M_4 and M_6. Although this contribution is of second-order, it can be relatively important depending on the values of the phase angles β and γ. Therefore, statements that the tidal-current constituents M_6, M_{10} *etc.* do not contribute to the tidally averaged bed-load transport (*e.g.* FRY & AUBREY, 1990) should be qualified.

The expression for the tidally averaged sediment flux, Eq. 12, is approximate in that terms of $O(\varepsilon^3)$ are neglected. In addition, deriving Eq. (12) involves evaluating contributions of the form

$$\frac{\varepsilon}{T}\int_{t_1 - T/2}^{t_1 + T/2} \cos\Delta\sigma t \cos^3\sigma t\, dt$$

The integral is approximated by

$$\frac{\varepsilon}{T}\cos\Delta\sigma t_1 \int_{t_1 - T/2}^{t_1 + T/2} \cos^3\sigma t\, dt$$

introducing an error in the dimensionless tidally averaged bed-load transport.

$$\varepsilon\frac{\Delta\sigma}{\sigma}\sin\Delta\sigma t_1\left[\frac{3}{4}\sin\sigma t_1 + \frac{1}{12}\sin 3\sigma t_1\right]$$

(eq. 14)

In Fig. 3, a comparison is made between the tidally averaged bed-load transport calculated from Eq. (12)

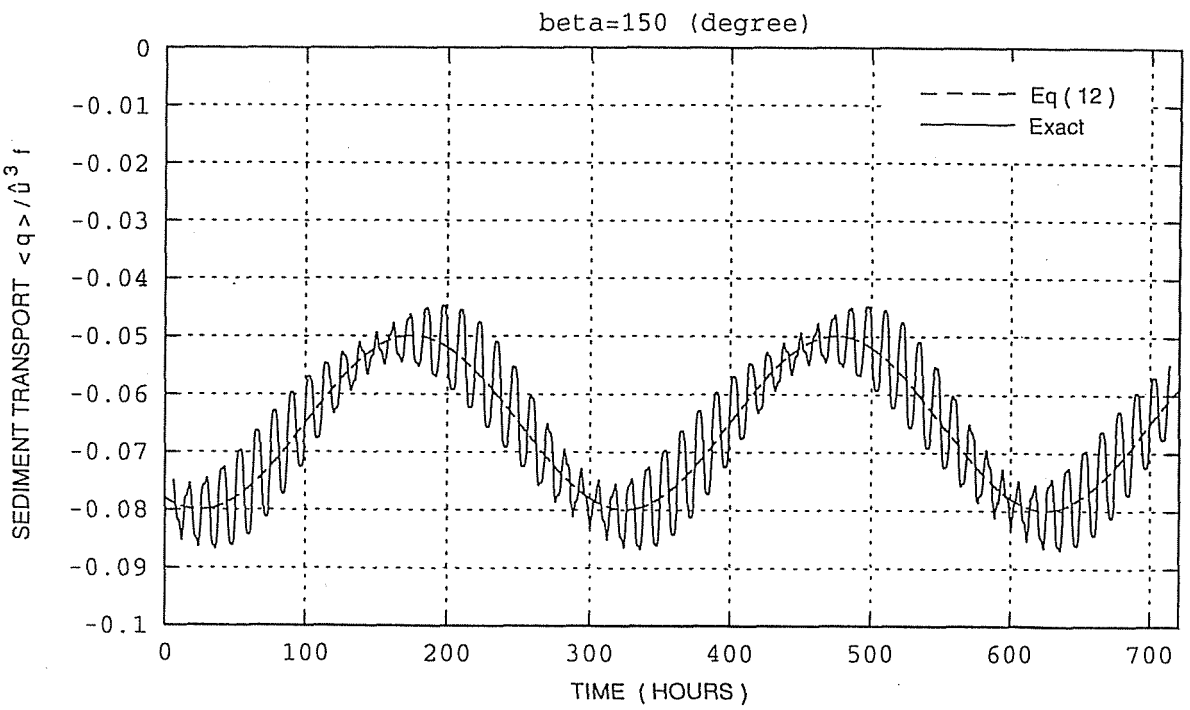

Fig. 3. Comparison of numerically and analytically (Eq. 12) calculated tidally averaged sediment transport; $\varepsilon_0=\varepsilon_6=0.0$, $\varepsilon_2=\varepsilon_4=\varepsilon_6=0.1$, $\beta=150°$, $\gamma=0°$.

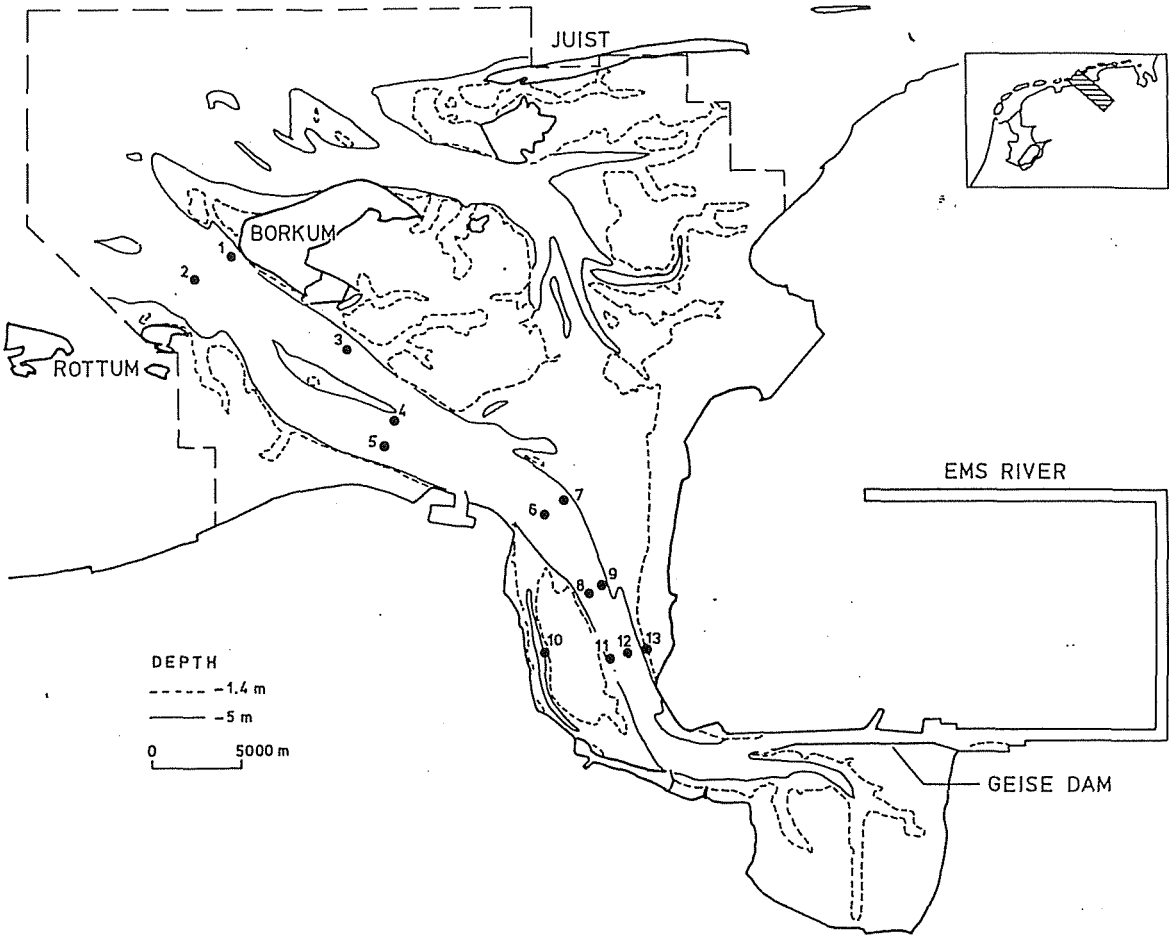

Fig. 4. Ems estuary; bathymetry, tidal-current stations and numerical model boundaries.

and the numerically calculated values using Eqs (5) and (8). Because of the error expressed by (14), the tidal fluctuations in the numerically calculated values are not present in the approximate analytical solutions. Note that in agreement with expression (14) the amplitude of the tidal variations varies with the beat frequency $\Delta\sigma$.

The analytical expression for the dimensionless tidally averaged bed-load transport for the set of tidal current constituents that include MS_4, N_2 and K_1 is presented in Appendix A. Compared to the results for the first set of tidal-current constituents a first-order contribution to the tidally averaged bed-load transport results from the interaction of M_2 and MS_4. Second-order tidally averaged sediment fluxes are introduced through the interaction of M_2 and K_1 and the triple interactions (M_2, M_0, N_2), (M_2, M_4, N_2), (M_2, M_6, MS_4), (M_2, S_2, MS_4) and (M_2, N_2, MS_4). Each of these fluxes fluctuates with the corresponding beat frequency and therefore does not contribute to the long-term mean bed-load transport.

The analytical expression for the long-term mean bed-load transport, Eq. (13), is based on the bed-load transport formula, Eq. (5), with n=3. Expressions for other values of n have the same general form as Eq. (13), with different coefficients. As an example for n=5 the expression for the first-order long-term mean bed-load flux is

$$\frac{\langle q \rangle}{\hat{u}^5 f} = \frac{15}{8}\varepsilon_c \qquad M_0, M_2$$

$$+\frac{5}{4}\varepsilon_2 \cos\beta \qquad M_4, M_2 \qquad \text{(eq. 15)}$$

From comparison with Eq. (13) it follows that the sediment transport resulting from the residual current becomes relatively more important when taking n=5.

The expressions for the net bed-load transport Eqs (13) and (15) are based on the premise that the instantaneous bed-load transport is proportional to some power of the local velocity. When taking the instantaneous bed-load transport proportional to some power of the bottom-shear stress, similar expressions for the net bed load can be derived. In that case the amplitudes and phases of the tidal current are replaced by the amplitudes and phases of the harmonic constituents of the bottom-shear stress.

5. APPLICATION TO THE EMS ESTUARY

a. Physical characteristics

The Ems estuary, situated along the Dutch-German border, is part of the Wadden Sea (Fig. 4). Its morphology is characterized by a main channel bordered by tidal flats. The part of the estuary that is of interest in this study is the main channel located between the current stations 11 and 12 and the island of Borkum. Channel widths and depths are typically 3000 m and 10 m, respectively. The bottom of the channel is covered with coarse sediment with local deposits of fine sediment. The water motion is dominated by the tide. The tide in the North Sea off the estuary is semi-diurnal. The principal water-level constituent is M_2 with an amplitude of 1 m. Maximum currents in the channel are 1 to 1.5 $m \cdot s^{-1}$. For the tidal-current station 12 in the Ems estuary, the amplitudes of the observed major tidal current constituents are plotted in Fig. 5. Although not an order of magnitude larger, M_2 is clearly the dominant harmonic. The mean daily discharge of the Ems river is 80 $m^3 \cdot s^{-1}$. In the area of interest waters are well mixed at all times and density currents can be neglected.

b. Numerical model

A two-dimensional vertically-averaged model was used to calculate the M_0, M_2, M_4 and M_6 tidal currents (ROBACZEWSKA *et al.*, 1992). The model covered the Ems estuary and the Ems river to the upstream dam; see Fig. 4. The open-sea boundaries were located one tidal excursion seaward of the island of Borkum. The lateral boundaries in the Wadden Sea were selected at the location of the high tidal flats between the islands of Rottum and Juist and the mainland and were treated as closed boundaries. The boundary at the upstream dam was treated as a discharge boundary.

The model area was covered with a 300x300 m square mesh. The full set of vertically-integrated non-linear equations of momentum (excluding the baroclinic term) and continuity were solved using an ADI finite-difference scheme (LEENDERTSE, 1967; STELLING, 1984). The time step in the model was 150 s. Along the open-sea boundary, water levels were prescribed in terms of harmonic constituents. These constituents were derived from a series of large-scale nested models. At the up-estuary boundary a constant discharge of 80 $m^3 \cdot s^{-1}$ was introduced.

The model was calibrated by adjusting the bottom-shear stress through the Mannings 'n' friction factor and comparing the amplitudes and phases of eight water-level constituents (O1, K1, N2, M2, S2, K2, M4 and M6) at seven stations. The amplitudes and phases of the harmonic constituents were determined from a one-month-long time series of calculated and observed water levels. Using a Mannings

$$n = 0.0225 \ s \cdot m^{-\frac{1}{3}},$$

good agreement was obtained between amplitudes and phases calculated in the model and from observations. For further details see ROBACZEWSKA *et al.* (1992).

c. Tidal-current constituents

Tidal currents were calculated for two sets of open-boundary conditions. The first set consisted of four water-level constituents: M_0, M_2, M_4 and M_6. The second set consisted of 26 water-level constituents, including M_0, M_2, M_4 and M_6. For the first set of boundary conditions the model was run till steady-state conditions were obtained, *i.e.* after about five tidal cycles. For the second set of boundary conditions the model was run for 30 days. For 13 selected stations the amplitudes and phases of the tidal constituents M_0, M_2, M_4 and M_6 for the along-channel current were determined using Fourier analysis and a least-square harmonic analysis. The 13 stations were located in the main channel of the estuary (Fig. 4). Except for stations 11 and 13, all stations were in the deeper relatively flat parts of the channel.

The magnitude and direction of M_0 and the ampli-

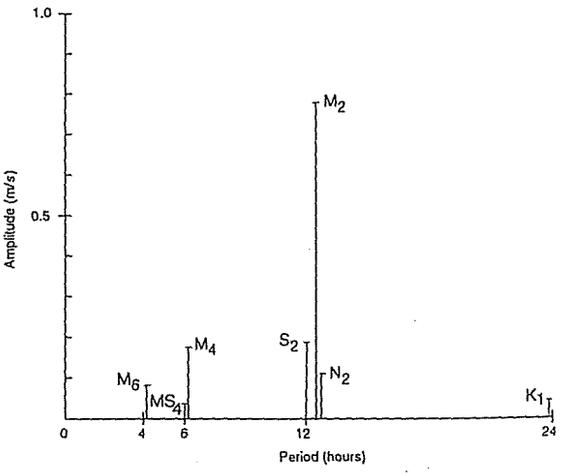

Fig. 5. Amplitudes of major tidal-current constituents in the Ems estuary determined from observations at station 12.

TABLE 1
Amplitudes and phases of the M_0, M_2, M_4 and M_6 tidal current.

	amplitude ($cm \cdot s^{-1}$)				phase (°)	
sta	M_0	M_2	M_4	M_6	β	γ
1	-4.0	119.4	5.1	10.1	263	241
2	9.1	99.8	2.7	8.7	288	241
3	-2.6	113.0	9.9	9.9	247	231
4	-8.7	90.0	11.4	9.6	279	250
5	0.7	73.0	7.2	7.4	281	231
6	-4.7	114.6	14.1	11.6	265	238
7	-3.6	82.2	12.1	7.0	260	243
8	-0.1	99.0	10.3	9.4	252	240
9	-1.4	105.0	16.1	14.6	268	250
10	-3.1	70.6	7.2	9.7	269	257
11	7.6	80.7	3.2	14.6	313	264
	(14.7)	(57.0)	(7.8)	(10.7)	(326)	(266)
12	-2.3	120.5	17.3	13.5	255	234
	(-0.7)	(76.6)	(17.0)	(7.0)	(237)	(234)
13	-4.2	97.6	14.6	14.3	263	247

( ) From observations at stations 11 and 12. For station 11 the amplitudes and phases are the average for the two current meters. For the Eulerian mean velocity at station 11 only the value of the upper current meter is available.
- ebb direction, + flood direction.

tudes and phases of M_2, M_4 and M_6 of the along-channel tidal current differed little for the two sets of open-boundary conditions. For the first set of open-boundary conditions the results of the Fourier analysis are presented in Table 1. Amplitudes of the M_2 tidal current were relatively uniform with values of about 1 $m \cdot s^{-1}$. Amplitudes of the M_4 and M_6 constituents were an order of magnitude smaller. Both showed a maximum of about 0.15 $m \cdot s^{-1}$ in the landward part of the study area. When excluding the shallow station 11, phase angles β varied between 247° and 293° resulting in relatively small values for cos β. Phase angles γ vary between 231° and 264°. Neither β nor γ show a definite trend with distance.

The magnitude of the Eulerian mean current in the 13 selected stations varies between ~0 $cm \cdot s^{-1}$ to ~15 $cm \cdot s^{-1}$.

Because of its relative importance for the tidally averaged bed-load transport (see section 5d,) the entire Eulerian-mean-velocity field is presented in Fig. 6. In the up-estuary part of the study area the velocity field is dominated by a set of headland eddies. The eddy south of Borkum is associated with ebb and flood channels in that area. Further seaward a pair of eddies that are typical of inlets, one turning in a clockwise and the other in an anti-clockwise direction, are recognized (RIDDERINKHOF, 1989). Overall the residual current pattern shows a strong spatial variation. This is in agreement with data from (13-hour) current measurements, presented by DE JONGE (1992).

Long-term current measurements in the study area were carried out in stations 11 and 12. The mean water depth at station 11 is 6 m. Current speed and direction were observed at two elevations: bottom + 0.25 m and bottom + 3.75 m. The mean water depth at station 12 is 12 m. A single current meter observing current speed and direction was located 1 m above the bottom. For both stations the data were analysed for the period 11 June 1990 - 15 July 1990. Amplitudes and phases of the along-channel current constituents derived from the observations are presented in brackets in Table 1. Observed and calculated amplitudes of M_2, M_4 and M_6 differed considerably. In part the reason for this is that the calculated values refer to vertically-averaged velocities smoothed over the width of the computational grid, whereas the measured values refer to a distinct position. For the same reason the magnitude of the observed and calculated Eulerian mean current should be expected to differ. Contrary to the amplitudes, the phase angles β and γ showed a much better agreement. In spite of the limited verification of the numerical model, it is felt that the calculated velocity field is sufficiently representative of the seaward part of the Ems estuary to arrive at qualitative conclusions with regard to the relative importance of tidal asymmetry and Eulerian mean current for the long-term mean bed-load transport.

d. The long-term mean bed-load transport

With the calculated values of the Eulerian mean current and amplitudes and phases of M_2, M_4 and M_6 listed in Table 1, the long-term mean bed-load transport for each of the 13 stations was calculated using Eq. (13). The contribution of each of the terms in Eq. (13) is listed in Table 2. For individual stations, whenever larger than ~3 $cm \cdot s^{-1}$, the Eulerian mean current is the major contributor to the long-term mean bed-

TABLE 2
Contributions of individual terms in Eq. (13) to the long-term mean bed-load transport. All values should be multiplied by 10^{-3}.

station	Term1 (M_2,M_0)	Term 2 (M_2,M_4)	Term 3 (M_2,M_4,M_6)	total
1	-50	-4	4	-50
2	138	6	2	146
3	-35	-26	12	-49
4	-146	15	18	-113
5	15	13	12	40
6	-63	-8	18	-53
7	-66	-19	18	-67
8	-9	-21	14	-16
9	-20	-6	26	0
10	-66	-1	20	-47
11	141	20	8	169
12	-29	-22	22	-29
13	-65	-14	32	-47

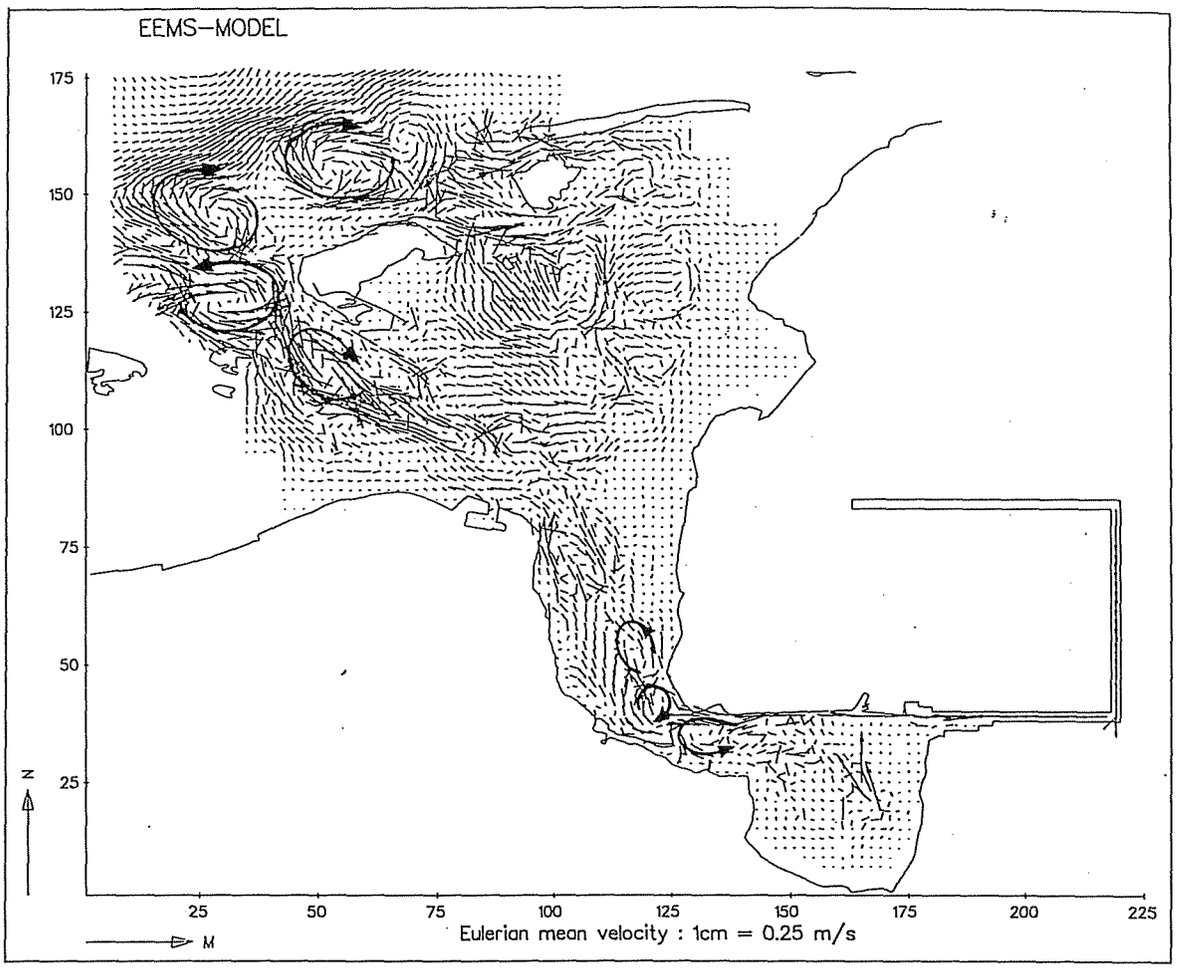

Fig. 6. Eulerian mean velocities.

load transport.

In Fig. 7 for each of the 13 stations the direction of the long-term mean bed-load transport is plotted together with the transport pathways of coarse sand estimated from known grain-size distributions of the bottom sediment (MCLAREN & BOWLES, 1985; MCLAREN, 1991). The agreement is encouraging. Except for stations 1 and 3, the directions of the bed-load transport were the same. Discrepancies should be expected due to the assumptions made in deriving Eq. (13) and the limited accuracy of the calculated velocity field and the sediment-transport pathways.

6. CONCLUSIONS

For a periodic tidal velocity, tidal asymmetry is defined in terms of the curve of demeaned current speed *versus* time. Tidal asymmetry exists when this curve is asymmetric with respect to times of slack water. A combination of a fundamental harmonic and any of its overtides, odd or even, results in tidal asymmetry.

Assuming the transport of coarse sediment (= bed-load transport) to be proportional to some power of the depth-averaged local current speed, it was shown that a combination of the M_2 tidal current and one of its even overtides leads to a tidally averaged bed-load transport. The direction of the net transport is determined by the phase of the overtide relative to the phase of the M_2 tidal current. A combination of the M_2 tidal current and one of its odd overtides leads to a zero tidally averaged transport of sediment.

Assuming M_2 to be the dominant tidal current constituent, an approximate analytical expression for the tidally averaged bed-load transport in a tidal channel was derived. The tidal current was assumed to be rectilinear and in addition to M_2 contained other fundamental constituents as well as the overtides and compound tides of M_2 and the Eulerian mean current (M_0). From the analytical expression it follows that the

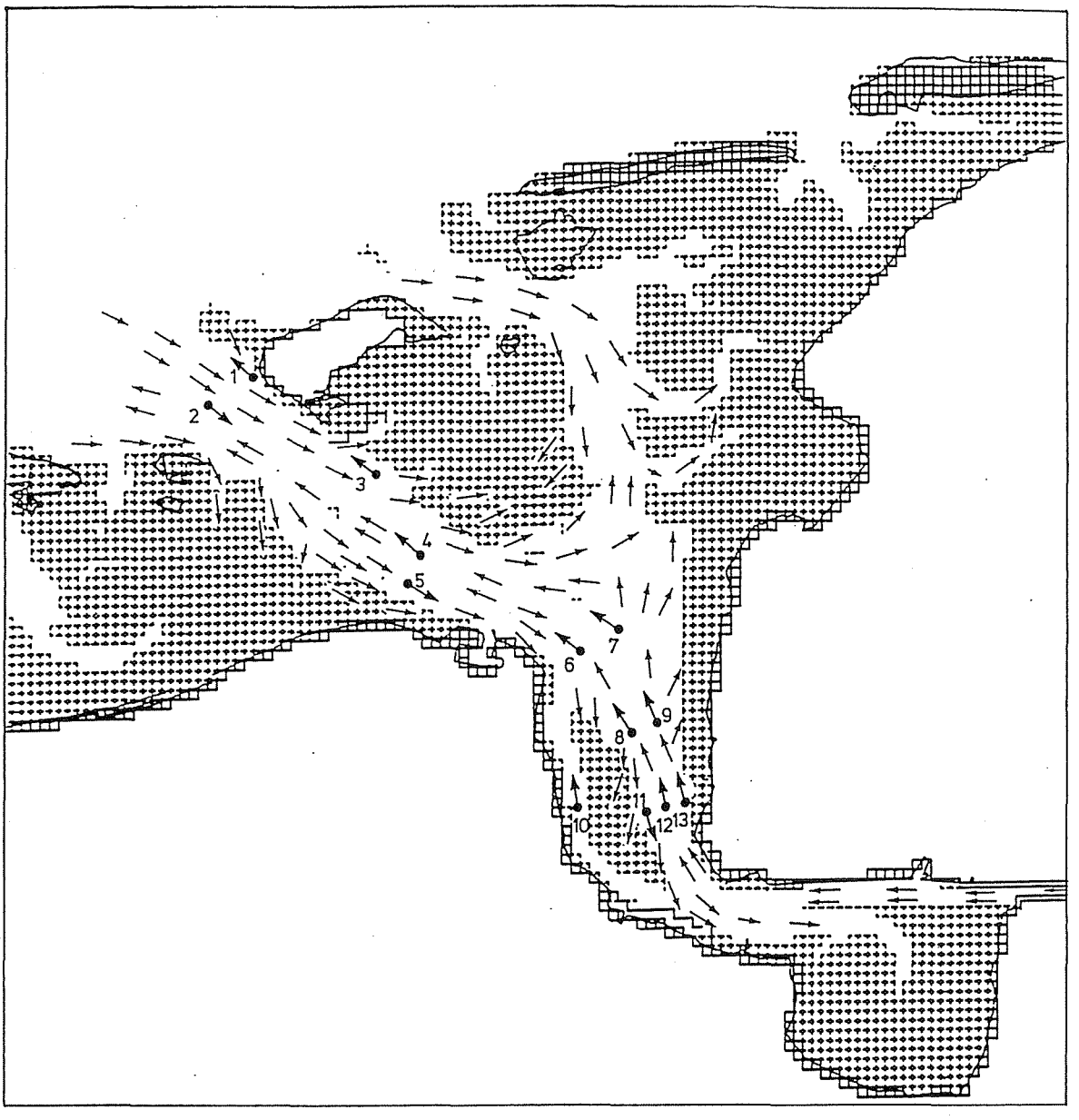

Fig. 7. Direction of long-term mean bed-load transport in the along-channel direction calculated from Eq. (13) and transport pathways derived from grain-size distribution patterns (MCLAREN, 1991).

interactions of M_2 and M_0 and M_2 and M_4 lead to a tidally averaged bed-load transport. The triple interaction of M_2, M_4 and M_6 causes a tidally averaged bed-load transport. The magnitude of this transport is an order smaller than that resulting from the interaction of M_2 and M_0 and M_2 and M_4. A combination of M_2 and a constituent in the diurnal, semi-diurnal and subsequent frequency bands results in a tidally averaged (over the M_2 period) transport having fluctuations with frequencies that are associated with the beat frequency of M_2 and the individual constituent. These beat frequencies correspond to periods in the 13-30 day period band. Therefore, for the long-term mean bed-load transport only M_0 and M_2 and its overtides are of importance.

Using the analytical expression, Eq. (13), the long-term mean bed-load transport was calculated for the main channels of the Ems estuary. The Eulerian

mean current and amplitudes and phases of the M_2, M_4 and M_6 tidal current are determined from a vertically integrated tidal model of the estuary. The bed-load transport is dominated by the interaction of the M_2 tidal current and the Eulerian mean current M_0. Comparison with bed-load transport pathways derived from grain-size distribution patterns shows good agreement.

7. PRACTICAL IMPLICATIONS

Many engineering studies in estuaries require the use of elaborate numerical sediment-transport models. Running these models for extended periods of time to cover a wide range of astronomical conditions is often cost prohibitive. Instead a periodic 'representative tide' is selected and the tidally averaged sediment transport corresponding to that tide is taken as representative of the long-term mean transport. Based on the results of this study it is concluded that the 'representative tide' should consist of M_0, M_2 and M_4. Here it is assumed that the sediment transport associated with the triple interactions between M_2, M_4 and M_6 is small. Among other things, this implies that the hydrodynamic part of the numerical transport models should be calibrated and verified using the M_0, M_2 and M_4 harmonics as a yardstick.

It is emphasized that the foregoing conclusions pertain to transport of coarse sediment by the astronomical tide including the tide-induced mean current. Furthermore, M_2 is assumed to be the dominant harmonic and the bed-load transport is taken proportional to some power of the local vertically-averaged velocity.

Results of computations with the hydrodynamic model of the Ems estuary show that the Eulerian mean current and the M_2, M_4 and M_6 tidal current constituents differ little when forcing the model at the open-sea boundary with M_0, M_2, M_4 and M_6 water-level constituents rather than the full suite of tidal harmonics. For practical applications this could be another cost-saving factor. With the periodic boundary conditions the model can be run until a steady state is reached. The M_0, M_2, M_4 and M_6 tidal current constituents follow from a simple Fourier analysis.

Disregarding wave action, in the seaward part of the Ems estuary the tidally averaged bed-load transport is dominated by the interaction of the M_2 tidal current and the Eulerian mean current. The same is expected to hold in the other tidal basins of the Wadden Sea. Therefore when not accounting for wave action the tidally averaged bed-load transport pattern is expected to closely resemble that of the Eulerian mean current.

Acknowledgement.—Support for the senior author was provided by the Tidal Waters Division of the Rijkswaterstaat under contract DYNASTAR-DG-439. Development of and computations with the hydrodynamic model of the Ems estuary was the responsibility of Ron P. van Dijk, Remco Plieger and Mohan Soerdjbali.

8. REFERENCES

AUBREY, D.G., 1986. Hydrodynamic controls on sediment transport in well-mixed bays and estuaries. In: J. VAN DE KREEKE. Physics of shallow estuaries and bays. Springer Verlag: 245-258.

BAGNOLD, R.A., 1966. An approach to the sediment problem from general physics. Geological Survey Professional Paper 422-I.

BOON, J.D. & R.J. BYRNE, 1981. On basin hypsometry and the morphodynamic response of coastal inlet systems.—Mar. Geol. **40:** 27-48.

DE JONGE, V.N., 1992. Tidal flow and residual flow in the Ems estuary.—Estuar. coast. Shelf Sci. **34:** 1-22.

DRONKERS, J., 1986. Tidal asymmetry and estuarine morphology.—Neth. J. Sea Res. **20:** 117-131.

FRIEDRICHS, C.T. & D.G. AUBREY, 1988. Non-linear tidal distortion in shallow well-mixed estuaries: A synthesis.—Estuar. coast. Shelf Sci. **27:** 521-545.

FRY, V.A. & D.G. AUBREY, 1990. Tidal velocity asymmetries and bed load transport in shallow embayments.—Estuari. coast. Shelf Sci. **30:** 453- 473.

LEENDERTSE, J.J., 1967. Aspects of a computational model for long-period wave propagation Rand Corporation, Memorandum RM-5294-PR. Santa Monica: 1-165.

MCLAREN, P., 1991. Sediment transport pathways in the Ems estuary. In: Rijkswaterstaat Nota GWWS-91.002.

MCLAREN, P. & D. BOWLES, 1985. The effects of sediment transport on grain- size distributions.—J. Sedim. Petrol. **55:** 0457- 0470.

PINGREE, R.D. & D.K. GRIFFITHS, 1979. Sand transport paths around the British Isles resulting from M_2 and M_4 tidal interactions.—J. mar. biol. Ass. U.K. **59:** 497-513.

RIDDERINKHOF, H., 1989. Tidal and residual flows in the western Dutch Wadden Sea, III: Vorticity balances.—Neth. J. Sea Res. **25:** 9-26.

ROBACZEWSKA, K.B., R.P. VAN DIJK, R. PLIEGER & M. SOERDJBALI, 1992. 'EEMS' - A hydrodynamics and waterquality model for the Ems-Dollard Estuary. Rijkswaterstaat DGW-92.010: 1-19.

STELLING, G.S., 1984. On the construction of computational methods for shallow water problems. Rijkswaterstaat, The Hague, Rijkswaterstaat Communications **35:** 1-226.

(accepted 20 July 1993)

APPENDIX A

Expression for dimensionless tidally averaged bed-load transport.

$$\frac{\langle q \rangle}{\hat{u}^3 f} = \frac{3}{2}\varepsilon_0 \qquad M_0, M_2$$

$$+ \frac{3}{4}\varepsilon_4 \cos\beta \qquad M_4, M_2$$

$$+ \frac{3}{2}\varepsilon_4 \varepsilon_6 \cos(\beta - \gamma) \qquad M_4, M_6, M_2$$

$+ \frac{3}{2} \varepsilon_4 \varepsilon_2 \cos(\Delta \sigma_1 t + \beta - \alpha_1)$ S_2, M_4, M_2

$+ 3 \varepsilon_2 \varepsilon_0 \cos(\Delta \sigma_1 t - \alpha_1)$ S_2, M_0, M_2

$+ \frac{3}{2} \varepsilon_4 \varepsilon_3 \cos(\Delta \sigma_2 t + \beta - \alpha_2)$ N_2, M_4, M_2

$+ 3 \varepsilon_3 \varepsilon_0 \cos(\Delta \sigma_2 t - \alpha_2)$ N_2, M_0, M_2

$+ \frac{3}{4} \varepsilon_5 \cos(\Delta \sigma_3 t - \beta_2)$ MS_4, M_2

$+ \frac{3}{2} \varepsilon_5 \varepsilon_6 \cos(\Delta \sigma_3 t + \gamma - \beta_2)$ MS_4, M_6, M_2

$+ \frac{3}{2} \varepsilon_5 \varepsilon_2 \cos(\Delta \sigma_3 t + \alpha_1 - \beta_2)$ MS_4, S_2, M_2

$+ \frac{3}{2} \varepsilon_5 \varepsilon_3 \cos(\Delta \sigma_3 t + \alpha_2 - \beta_2)$ MS_4, N_2, M_2

$+ \frac{3}{4} \varepsilon_7^2 \cos 2(\Delta \sigma_4 t - \delta)$ K_1, M_2

$+ 0(\varepsilon^3)$

for

$u/\hat{u} = \varepsilon_0 + \cos \sigma t + \varepsilon_4 \cos(2 \sigma t - \beta) + \varepsilon_6 \cos(3 \sigma t - \gamma)$

$+ \varepsilon_2 \cos(\sigma_1 t - \alpha_1) + \varepsilon_3 \cos(\sigma_2 t - \alpha_2)$

$+ \varepsilon_5 \cos(\sigma_3 t - \beta_2) + \varepsilon_7 \cos(\sigma_4 t - \delta)$

with

$\sigma_1 - \sigma = \Delta\sigma_1$
$\sigma - \sigma_2 = \Delta\sigma_2$
$\sigma_3 - 2\sigma = \Delta\sigma_3$
$2\sigma_4 - \sigma = \Delta\sigma_4$

Note: When including the diurnal tide constituent, tidal average (<>) implies the average over two times the M_2 period.